

Using the boundary conditions, namely

$$\begin{aligned} x = 0, \quad T &= T_0(t) \\ x = \beta(t), \quad T &= 0 \end{aligned}$$

together with the smoothing conditions

$$\begin{aligned} x = \beta, \quad \left(\frac{\partial T}{\partial x} \right) &= 0 \\ x = \beta, \quad \left(\frac{\partial^2 T}{\partial x^2} \right) &= 0 \end{aligned} \quad (13)$$

we determine the following simple polynomial function to represent the temperature distribution inside the unsteady thermal boundary layer:

$$T/T_0 = 1 - 3x/\beta + 3x^2/\beta^2 - x^3/\beta^3, \quad (0 \leq x \leq \beta) \quad (14)$$

Here, β is the variational parameter to be determined by the analysis. Substitution of the temperature distribution, Eq. (14), into the balance equation, Eq. (12), integration with respect to x , and evaluation of the constant of integration using the smoothing condition $\partial T^*/\partial x = 0$ at $x = \beta$, yields

$$\begin{aligned} \frac{\partial T^*}{\partial x} &= (T_0/\alpha)[a(x - 3x^2/2\beta + x^3/\beta^2 - x^4/4\beta^3 \\ &\quad - \beta/4)/t + \beta'(3x^2/2\beta^2 - 2x^3/\beta^3 + 3x^4/4\beta^4 - \frac{1}{4})] \\ &\quad (0 \leq x \leq \beta) \end{aligned} \quad (15)$$

where $\alpha (= \lambda/\rho C_v)$ is the thermal diffusivity, and the prime denotes the time derivative. With the help of the above flux expression and the temperature distribution, Eq. (14), the variational principle, Eq. (11), after integration with respect to x , reduces to the following form:

$$\begin{aligned} \delta \int_0^\infty \{ T_0^2 \beta [3a/28 + 5\beta' t/(28\beta)]/(\alpha t) - 9T_0^2/10\beta \\ - T_0^2 \beta^3 [a^2/288 + \beta'^2 t/(112\beta^2) \\ + a\beta' t/(96\beta)]/(t^2 \alpha^2) \} dt = 0 \end{aligned} \quad (16)$$

The variational parameter is β , and therefore, the Euler-Lagrange equation of this variational formulation is

$$\frac{\partial L}{\partial \beta} - \left(\frac{\partial L}{\partial \beta'} \right)' = 0 \quad (17)$$

if the variational principle (16) is written in the concise form

$$\delta \int_0^\infty L dt = 0 \quad (18)$$

using the Lagrangian density L . However, if we introduce β^* , the dimensionless thermal boundary-layer thickness, given by

$$\beta^* = \beta/\sqrt{\alpha t} \quad (19)$$

we obtain the Euler-Lagrange equation of the variational principle (16) as follows:

$$\frac{\partial L}{\partial \beta^*} = 0$$

or

$$\beta^{*4}(70a^2 + 105a + 45) - \beta^{*2}(720a + 600) - 6048 = 0 \quad (20)$$

Equation (20) is a quadratic equation in β^{*2} yielding solution for β^* for given values of the surface temperature power law time exponent a . The β^* solution thus obtained enables us to compute the temperature gradient inside the boundary layer with the help of Eq. (15). The dimensionless temperature gradient at the boundary surface is calculated with the help of the expression

$$\sqrt{(\alpha/T_0^2)} \left(-\frac{\partial T}{\partial x} \right)_{x=0} = \beta^*(a + 0.5)/4 \quad (21)$$

It is noted that the heat transfer at the boundary surface vanishes when the surface variation temperature exponent a assumes the value -0.5 ; this is consistent with the results of similarity theory which gives the corresponding surface temperature decay for the insulated surface situation.

The algebraic equation, Eq. (20), and local heat transfer expression, Eq. (21), constitute a complete analytical solution to the present unsteady heat conduction problem. Therefore, it is demonstrated by the present work that this unique approximate analytical method may be employed as a tool for solving heat transfer problems.

Acknowledgment

We gratefully thank the Associate Editor for his critical evaluation of the manuscript.

References

- ¹Gyarmati, I., "On the 'Governing Principle of Dissipative Processes' and Its Extension to Non-Linear Problems," *Annual Physics Review*, Vol. 23, No. 7, 1969, pp. 353-378.
- ²Gyarmati, I., *Non-Equilibrium Thermodynamics, Field Theory and Variational Principles*, 1st ed., Springer-Verlag, Berlin, 1970, pp. 133-141.
- ³Stark, A., "Approximate Methods for the Solution of Heat Conduction Problems Using Gyarmati's Principle," *Annual Physics Review*, Vol. 31, No. 1, 1974, pp. 53-75.

Refractive Index Effects on Local Radiative Emission from a Rectangular Semitransparent Solid

Robert Siegel*

NASA Lewis Research Center, Cleveland, Ohio 44135

Introduction

LOCAL radiant emission from a two-dimensional rectangular solid at uniform temperature is analyzed when the solid refractive index n is greater than 1. Since internal emission depends on n^2 , a large n can provide internal radiation much larger than blackbody radiation emitted into a vacuum. Blackbody emission from the boundary is not exceeded because of internal reflection of part of the outward-directed energy at the boundary, primarily by total reflection. Energy

Received July 2, 1993; revision received Oct. 18, 1993; accepted for publication Oct. 19, 1993. Copyright © 1993 by the American Institute of Aeronautics and Astronautics, Inc. No copyright is asserted in the United States under Title 17, U.S. Code. The U.S. Government has a royalty-free license to exercise all rights under the copyright claimed herein for Governmental purposes. All other rights are reserved by the copyright owner.

*Senior Research Scientist, Lewis Research Academy, 21000 Brookpark Road, Fellow AIAA.

reaching the boundaries, and reflected energy are both assumed diffuse.

Most analyses in the literature for radiating materials with $n > 1$ are for plane layers. In a paper¹ related to the present work, radiation from a corner and a semi-infinite slab were obtained with specular boundaries. The present analysis determines radiating characteristics of a solid with diffuse boundaries and a rectangular cross section; the third dimension is long, and so behavior is two-dimensional. The required equations are derived by starting with expressions from Siegel^{2,3} for an absorbing and emitting rectangular medium with $n = 1$. This provides local boundary heat fluxes from a radiating medium at uniform temperature, and from enclosing black boundaries, each at a different uniform temperature, that radiate to each other through the medium. By adding n^2 factors to the emission terms in Ref. 2, the relations provide the emitted fluxes from the medium that are incident on the boundary. The expressions in Ref. 3 provide the coupling between local positions on the boundary produced by internal reflections. This leads to a formulation for the radiated flux locally transmitted through the boundary. For convenience the analysis is carried out for a gray solid, but the local emittances can also be applied for spectrally dependent calculations.

Analysis

A rectangular region, $0 \leq x \leq d$ and $0 \leq y \leq b$ ($d > b$, aspect ratio $A_R = d/b$), is a semitransparent solid at uniform temperature T_M . There are no surrounding walls, therefore the sides are directly exposed to an environment at T_E . The solid refractive index is n ; for the environment, $n_E = 1$. The geometry is long normal to the x - y plane, and so its behavior is two-dimensional. For convenience the derivation is for a gray solid (absorption coefficient a), but the results for local emittance along the sides are valid spectrally by using the emittance corresponding to a_λ at each λ . The derivation is carried out initially for $T_E = 0$; then, since the solid is at uniform temperature, the relations are readily extended for $T_E > 0$.

The energy that leaves the rectangle through its boundary at a local position is obtained in two parts: energy directly emitted from within the solid, and energy reflected internally along the boundary and then reaching the location being considered. For the first of these, using the relations in Ref. 2, the flux emitted from a two-dimensional gray rectangular medium to a local position, $X = x/b$, along its long side at $Y = y/b = 1$ is

$$q_{M-L}(X) = n^2 \sigma T_M^4 \left\{ 1 - S_{1-3}(BX) - S_{1-3}[B(A_R - X)] - B \int_{X'=0}^{A_R} S_{0-2}[BR_1(X, X')] dX' \right\} \quad (1a)$$

where $R_1(X, X') = [(X - X')^2 + 1]^{1/2}$, and $B = ab$ (optical thickness of short side). The notation is $S_{1-3} = S_1 - S_3$ and $S_{0-2} = S_0 - S_2$, where the S_n are integral functions in two-dimensional radiative transfer.^{4,5}

Since the solid has $n > 1$, there are reflections at the internal interface of the boundary. The local energy fluxes incident (with flux q_i) upon, and leaving, the internal interface are assumed diffuse; the internal diffuse reflectivity is ρ^i . The internal flux leaving position X on the long side at $Y = 0$ is reflected incident flux, $\rho^i q_i(X)$. The flux incident at X on the long side at $Y = 1$, by transmission through the solid of reflected energy from the entire interface of the opposite long side, is then³

$$q_{L-L}(X) = \rho^i \int_{X'=0}^{A_R} q_i(X') \frac{S_3[BR_1(X, X')]}{R_1(X, X')^3} dX' \quad (1b)$$

In a similar fashion Eq. (1c) is the local flux incident internally on the long side at $Y = 1$ by energy reflected internally from the interfaces of the two short sides and then transmitted through the medium

$$q_{S-L}(X) = \rho^i \left[X \int_{Y=0}^1 q_i(Y) \frac{1-Y}{R_2(X, Y)^3} S_3[BR_2(X, Y)] dY + (A_R - X) \int_{Y=0}^1 q_i(Y) \frac{1-Y}{R_3(X, Y)^3} S_3[BR_3(X, Y)] dY \right] \quad (1c)$$

where $R_2(X, Y) = [X^2 + (1 - Y)^2]^{1/2}$ and $R_3(X, Y) = [(A_R - X)^2 + (1 - Y)^2]^{1/2}$.

The heat fluxes in Eqs. (1a-1c) are added, and their sum, $q_i(X) = q_{M+L}(X) + q_{L-L}(X) + q_{S-L}(X)$ is the incident flux at local X position on the interior of the long side at $Y = 1$

$$q_i(X) = n^2 \sigma T_M^4 \left\{ 1 - S_{1-3}(BX) - S_{1-3}[B(A_R - X)] - B \int_{X'=0}^{A_R} S_{0-2}[BR_1(X, X')] dX' \right\} + \rho^i \left[\int_{X'=0}^{A_R} q_i(X') \frac{S_3[BR_1(X, X')]}{R_1(X, X')^3} dX' + X \int_{Y=0}^1 q_i(Y) \frac{1-Y}{R_2(X, Y)^3} S_3[BR_2(X, Y)] dY + (A_R - X) \int_{Y=0}^1 q_i(Y) \frac{1-Y}{R_3(X, Y)^3} S_3[BR_3(X, Y)] dY \right] \quad (2)$$

Since $q_i(X)$ is in the integrals on the right side of Eq. (2), this equation—along with a similar relation for the short side—provide a pair of coupled integral equations for $q_i(X)$ and $q_i(Y)$ along the internal interfaces of the rectangle sides.

The locally emitted flux leaving the exterior surface equals the flux incident internally on the boundary and then transmitted through the surface, $q_e = (1 - \rho^i)q_i$. By using this relation to eliminate q_i in Eq. (2), and place it in terms of q_e , an integral equation is obtained relating the local emittance $\epsilon_L(X) = q_e(X)/\sigma T_M^4$ along the long side, $Y = 1$, to the local emittances along the other sides:

$$\epsilon_L(X) = n^2(1 - \rho^i) \left\{ 1 - S_{1-3}(BX) - S_{1-3}[B(A_R - X)] - B \int_{X'=0}^{A_R} S_{0-2}[BR_1(X, X')] dX' \right\} + \rho^i \left[\int_{X'=0}^{A_R} \epsilon_L(X') \frac{S_3[BR_1(X, X')]}{R_1(X, X')^3} dX' + X \int_{Y=0}^1 \epsilon_S(Y) \frac{1-Y}{R_2(X, Y)^3} S_3[BR_2(X, Y)] dY + (A_R - X) \int_{Y=0}^1 \epsilon_S(Y) \frac{1-Y}{R_3(X, Y)^3} S_3[BR_3(X, Y)] dY \right] \quad (3a)$$

Similarly, the local emittance along the short side at $X = d/b = A_R$ is

$$\begin{aligned} \varepsilon_s(Y) = & n^2(1 - \rho^i) \left\{ 1 - S_{1-3}(BY) - S_{1-3}[B(1 - Y)] \right. \\ & \left. - B \int_{Y'=0}^1 S_{0-2}[BR_4(Y, Y')] dY' \right\} \\ & + \rho^i \left[A_R^2 \int_{Y'=0}^1 \varepsilon_s(Y') \frac{S_3[BR_4(Y, Y')]}{R_4(Y, Y')^3} dY' \right. \\ & + Y \int_{X=0}^1 \varepsilon_L(X) \frac{A_R - X}{R_5(X, Y)^3} S_3[BR_5(X, Y)] dX \\ & \left. + (1 - Y) \int_{X=0}^{A_R} \varepsilon_L(X) \frac{A_R - X}{R_5(X, Y)^3} S_3[BR_3(X, Y)] dX \right] \end{aligned} \quad (3b)$$

where $R_4(Y, Y') = [A_R^2 + (Y - Y')^2]^{1/2}$ and $R_5(X, Y) = [(A_R - X)^2 + Y^2]^{1/2}$.

After the simultaneous integral equations in Eqs. (3a) and (3b) are solved numerically for $\varepsilon_L(X)$ and $\varepsilon_s(Y)$, the overall emittance of the rectangle is obtained by integrating the energy leaving the boundary

$$\varepsilon_R = \frac{1}{1 + A_R} \left[\int_0^{A_R} \varepsilon_L(X) dX + \int_0^1 \varepsilon_s(Y) dY \right] \quad (4)$$

The emittances were derived for $T_E = 0$. Since the solid is at uniform temperature, the emittances remain the same when $T_E > 0$. Then, for example, the net local heat loss at a position on the long side is $q_L(X) = \varepsilon_L(B, X, A_R) \sigma (T_M^4 - T_E^4)$.

To extend the results to a nongray medium, the emittances are applied spectrally.⁶ For a spectrally emitting medium $B_\lambda = a_\lambda b$, and the local spectral flux in wavelength interval $d\lambda$ emitted through the boundary is $dq_{\lambda,L}(X) = \varepsilon_{\lambda,L}(B_\lambda, X, A_R) e_{\lambda b}(\lambda, T_M) d\lambda$, where $e_{\lambda b}$ is the blackbody function. By integrating over all wavelengths, the net flux lost at a position on the long side is

$$q_L(X) = \int_0^\infty \varepsilon_{\lambda,L}(B_\lambda, X, A_R) [e_{\lambda b}(\lambda, T_M) - e_{\lambda b}(\lambda, T_E)] d\lambda \quad (5)$$

The net heat loss from the entire rectangle is

$$q_R = \int_0^\infty \varepsilon_{\lambda,R}(B_\lambda, A_R) [e_{\lambda b}(\lambda, T_M) - e_{\lambda b}(\lambda, T_E)] d\lambda \quad (6)$$

where $\varepsilon_{\lambda,R}(B_\lambda, A_R) = \varepsilon_R(B, A_R)$ from Eq. (4) with $B_\lambda = B$.

The diffuse reflectivity ρ^i on the inside of the surface needed for solving Eqs. (3a) and (3b) is given by the Fresnel relation⁵

$$\begin{aligned} \rho^i = & 1 - \frac{1}{2n^2} + \frac{(3n + 1)(n - 1)}{6n^2(n + 1)^2} \\ & + \frac{(n^2 - 1)^2}{(n^2 + 1)^3} \left[\frac{(n - 1)}{(n + 1)} - \frac{2n(n^2 + 2n - 1)}{(n^2 + 1)(n^4 - 1)} \right] \\ & + \frac{8n^2(n^4 + 1)}{(n^2 + 1)(n^4 - 1)^2} \left[\frac{1}{n} \right] \end{aligned} \quad (7)$$

The simultaneous integral equations in Eqs. (3a) and (3b) were solved numerically. When $n = 1$ there are no internal reflections, and only the first four terms are on the right side. Results for $n = 1$ from Ref. 2 were used to begin solving with $n > 1$. An iterative method was used by placing this approximation into the right sides of Eqs. (3a) and (3b) and integrating to obtain values for the next iteration. The $\varepsilon_L(X)$

and $\varepsilon_s(Y)$ were evaluated at unevenly spaced intervals along the boundary with more closely spaced points near the corner. Cubic splines were used for the ε and S_n values to interpolate intermediate values of the integrands needed in the integration subroutine. The method converged to ε values within 0.001 with 25 iterations or less.

One of the integrals is singular at a corner and requires special evaluation. With R_2 inserted, the third integral on the right side of Eq. (3a) is

$$I(X) \equiv X \int_{Y=0}^1 \varepsilon_s(Y) \frac{1 - Y}{[X^2 + (1 - Y)^2]^{3/2}} \times S_3[B(X^2 + (1 - Y)^2)^{1/2}] dY \quad (8)$$

The $I(X) = 0$ when $X = 0$, except at the corner $Y = 1$, where $I(X)$ has zeros in both numerator and denominator. In the limit, $X \rightarrow 0$, $Y \rightarrow 1$, the argument of S_3 is zero giving $S_3(0) = \frac{1}{2}$. Then, with the change of variable, $\xi = 1 - Y$

$$I(0) = \lim_{X \rightarrow 0} \left[\varepsilon_s(1) \frac{X}{2} \int_{\xi=0}^\Delta \frac{\xi}{(X^2 + \xi^2)^{3/2}} d\xi \right]$$

where Δ is small. The integral is evaluated analytically, and with Δ and X equal to zero, $I(0) = \varepsilon_s(1)/2$. This replaces $I(X)$ when evaluating $\varepsilon_L(0)$ from Eq. (3a).

Results and Discussion

Local emittances for a square, and a rectangle with $A_R = 2$, are in Figs. 1 and 2 for $n = 1$ to 3, and $a_\lambda b = B_\lambda$ from 0.2 to 4. The integrated average ε_R are in Fig. 3. By using these emittances the net energy lost from the entire boundary is computed from Eq. (6) when the surroundings are at uniform temperature T_E .

The local emittance along one-half of one side of a square is in Fig. 1 as a function of n for $a_\lambda b = 0.2, 1$, and 4. When the optical thickness is small, $a_\lambda b = 0.2$ (dot-dashed lines), the emittance is fairly uniform across each side of the square when $n = 1$. As n is increased, the local ε_λ increases substantially at all locations along the side and its uniformity is increased. For a larger optical thickness, $a_\lambda b = 4$ (dashed lines), the behavior with increasing n differs from that for small $a_\lambda b$. When $n = 1$, ε_λ is substantially smaller near the corner than along the central portion of the side. The local ε_λ do not increase uniformly with increasing n . At the corner

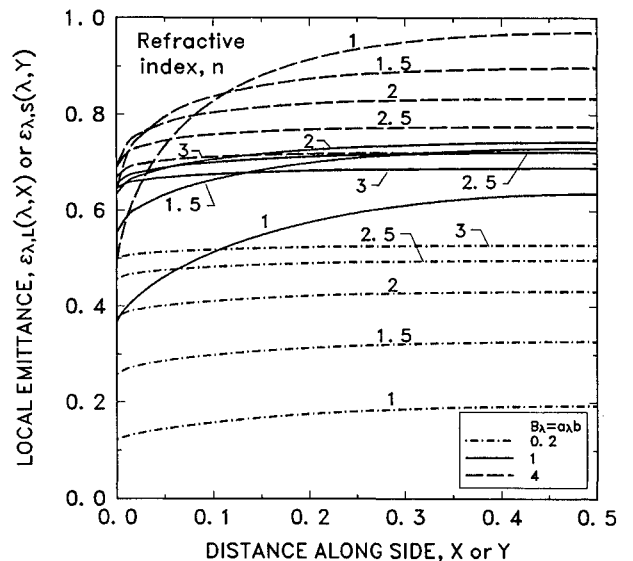


Fig. 1 Local emittances from the sides of a two-dimensional solid with a square cross section, as a function of its refractive index and the optical thickness of a side.

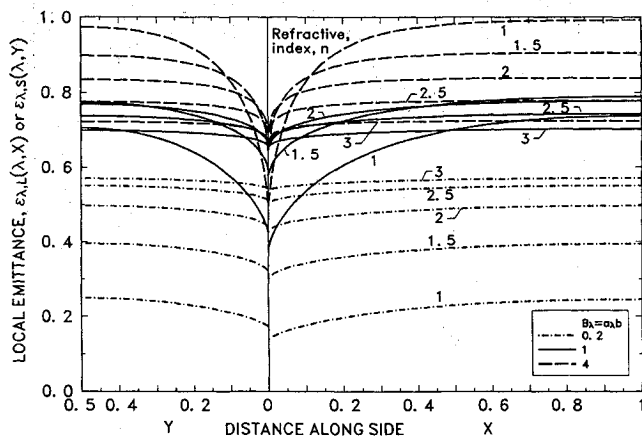


Fig. 2 Local emittances from the sides of a two-dimensional solid with a rectangular cross section of aspect ratio 2, as a function of its refractive index and the optical thickness of the short side.

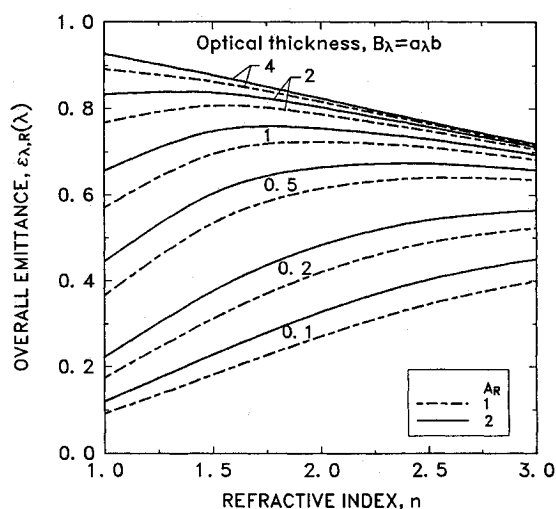


Fig. 3 Integrated average emittance from a two-dimensional rectangular solid with aspect ratios 1 and 2 as a function of its refractive index and the optical thickness of the short side.

they increase for n up to about 2.5; they then decrease as n becomes larger. At the center of the side, ϵ_λ decreases with increasing n . As n is increased, the emittance becomes more uniform across the side.

Figure 2 gives local ϵ_λ along the short and long sides of a rectangle with $A_R = 2$. The $\epsilon_L(X)$ and $\epsilon_S(Y)$ behavior with n and $a_\lambda b$ is similar to Fig. 1. At the corner there is a small difference in the local emittances on the two sides. This difference is very small when either n or $a_\lambda b$ is large. For large $a_\lambda b$ the behavior in the corner region becomes radiatively isolated from the other parts of the volume; the $\epsilon_L(X)$ and $\epsilon_S(Y)$ variations along the two sides tend to become the same in the corner region.

The integrated average emittances are in Fig. 3 as a function of refractive index for $A_R = 1$ and 2; these can be used to compute the overall heat loss for any T_M and T_E , and for a spectral variation of a_λ . The trends are in accord with those in Figs. 1 and 2. For small $a_\lambda b$, the overall spectral emittance $\epsilon_{\lambda,R}(\lambda)$ increases as n is increased. For a large $a_\lambda b$ this trend is reversed. For intermediate $a_\lambda b$, the overall emittance passes through a maximum with increasing n .

Conclusions

Local and integrated average spectral emittances are obtained around the boundary of a two-dimensional rectangular solid at uniform temperature and with a refractive index larger than one. Radiation at the boundaries is assumed diffuse, and

internal reflections are included. The results show the effect on emittance of refractive index, optical thickness $a_\lambda b$, and aspect ratio. For an optically thin region with $a_\lambda b$ less than about 1, the local and overall emission increase as refractive index increases. For $a_\lambda b$ larger than about 2.5 the trend is reversed, and so increasing n results in decreased emission. The minimum local emittance occurs at the corners. An increased refractive index causes the local emittance to be more uniform over each side of the rectangle.

References

- Wu, C. Y., Sutton, W. H., and Love, T. J., "Directional Emittance of a Two-Dimensional Scattering Medium with Fresnel Boundaries," *Journal of Thermophysics and Heat Transfer*, Vol. 3, No. 3, 1989, pp. 274–282.
- Siegel, R., "Analytical Solution for Boundary Heat Fluxes from a Radiating Rectangular Medium," *Journal of Heat Transfer*, Vol. 113, No. 1, 1991, pp. 258–261.
- Siegel, R., "Relations for Local Radiative Heat Transfer Between Rectangular Boundaries of an Absorbing-Emitting Medium," *Journal of Heat Transfer*, Vol. 115, No. 1, 1993, pp. 272–276.
- Yuen, W. W., and Wong, L. W., "Numerical Computation of an Important Integral Function in Two-Dimensional Radiative Transfer," *Journal of Quantitative Spectroscopy and Radiative Transfer*, Vol. 29, No. 2, 1983, pp. 145–149.
- Siegel, R., and Howell, J. R., *Thermal Radiation Heat Transfer*, 3rd ed., Hemisphere, Washington, DC, 1992.
- Siegel, R., "Boundary Heat Fluxes for Spectral Radiation from a Uniform Temperature Rectangular Medium," *Journal of Thermophysics and Heat Transfer*, Vol. 6, No. 3, 1992, pp. 543–545.

Surface Radiation for Rectangular Enclosures Using the Discrete-Ordinates Method

J. R. Ehlert* and T. F. Smith†

University of Iowa, Iowa City, Iowa 52242

Introduction

SÁNCHEZ and Smith¹ formulated the discrete-ordinates method (DOM) for radiant exchange between surfaces separated by a transparent medium for a two-dimensional geometry and demonstrated that the DOM predicted accurate heat fluxes when compared to those of the radiosity/irradiation method (RIM). The purpose of this study is to apply the DOM to compute the radiant exchange for a three-dimensional rectangular enclosure. The formulation is based on that provided by Sánchez and Smith.

Analysis

The rectangular enclosure has lengths of $L_{x,y,z}$ for the x , y , and z axes. The enclosure may contain protrusions and obstructions. The enclosure surfaces, protrusions, and obstructions are diffusely emitting and reflecting, are radiatively opaque, and may have nonuniform radiative property and temperature distributions. The radiative properties are independent of temperature, although this may be relaxed. Openings in the enclosure walls, if present, are represented

Received Aug. 12, 1993; revision received Dec. 3, 1993; accepted for publication Dec. 3, 1993. Copyright © 1993 by the American Institute of Aeronautics and Astronautics, Inc. All rights reserved.

*Research Assistant, Department of Mechanical Engineering.

†Professor, Department of Mechanical Engineering. Senior Member AIAA.